ORIGINAL ARTICLE

Oral Science International
Official Journal of the Japanese Stomatological Society

WILEY

Quantification of three-dimensional morphology of craniofacial mineralized tissue defects in Tgfbr2/Osx-Cre mice

Taylor Nicholas Snider[1] | Ke'ale W. Louie[1] | Gabrielle Zuzo[1] |
Antonio Carlos de Oliveira Ruellas[2] | Richard Christian Solem[2] |
Lucia H. S. Cevidanes[2] | Honghao Zhang[1] | Yuji Mishina[1] (iD)

[1]Department of Biologic and Materials Sciences & Prosthodontics, School of Dentistry, University of Michigan, Ann Arbor, MI, USA

[2]Department of Pediatric and Orthodontic Dentistry, School of Dentistry, University of Michigan, Ann Arbor, MI, USA

Correspondence
Honghao Zhang and Yuji Mishina, Department of Biologic and Materials Sciences & Prosthodontics, School of Dentistry, University of Michigan, 4222A Dental, 1011 N. University Ave, Ann Arbor, MI 48109-1078, USA.
Email: zhangho@umich.edu (H. Z.) and mishina@umich.edu (Y. M.)

Abstract

Craniofacial morphology is affected by the growth, development, and three-dimensional (3D) relationship of mineralized structures including the skull, jaws, and teeth. Despite fulfilling different purposes within this region, cranial bones and tooth dentin are derived from mesenchymal cells that are affected by perturbations within the TGF-β signaling pathway. *TGFBR2* encodes a transmembrane receptor that is part of the canonical, SMAD-dependent TGF-β signaling pathway and mutations within this gene are associated with Loeys-Dietz syndrome, a condition which often presents with craniofacial signs including craniosynostosis and cleft palate. To investigate the role of *Tgfbr2* in immature, but committed, mineralized tissue forming cells, we analyzed postnatal craniofacial morphology in mice with conditional *Tgfbr2* deletion in *Osx*-expressing cells. Novel application of a 3D shape-based comparative technique revealed that *Tgfbr2* in *Osx*-expressing cells results in impaired postnatal molar root and anterior cranial growth. These findings support those from studies using similar *Tgfbr2* conditional knockout models, highlight the anomalous facial and dental regions/structures using tomographic imaging-based techniques, and provide insight into the role of *Tgfbr2* during postnatal craniofacial development.

KEYWORDS
3D modeling, morphometry, Tgfbr2, tissue engineering

1 | INTRODUCTION

Growth and development of specialized structures within the craniofacial complex require dynamic coordination between the cells of multiple organs and tissues. Among these elements are the teeth, jaws, and cranial skeleton, all mineralized structures which significantly affect function (*eg*, communication and eating) and appearance (*eg*, facial profile, proportions, and symmetry) within this region. Craniofacial morphology of human patients can be quantitatively described via cephalometric analyses that rely on linear and angular measurements between standardized radiographic landmarks.[1,2]

However, reduced dimensionality (*ie*, from three to two dimensions) may obscure critical shape-based differences in complete structures. Volume rendering from tomographic imaging (*eg*, CT, MRI, or μCT) circumvents this issue by permitting three-dimensional (3D) shape-based comparisons that provide detailed insight into the etiology of anomalous craniofacial states.

Among the most common birth defects, the genetic cause of many craniofacial anomalies remains unknown. However, mutations in *TGFBR2* have been associated with Loeys-Dietz syndrome, a condition which can present with connective tissue defects and craniofacial signs including craniosynostosis and cleft palate.[3,4] *TGFBR2* is part of the canonical, SMAD-dependent TGF-β signaling pathway and encodes a constitutively active transmembrane serine/

threonine tyrosine kinase receptor that initiates downstream signaling by forming a heterotetrameric complex with *TGFBR1*.[5] The TGF-β superfamily encompasses two receptor types and multiple ligands such as TGF-βs (*eg*, TGF-β1, TGF-β2, TGF-β3), bone morphogenetic proteins (BMPs), activins, and growth and differentiation factors (GDFs) that interact with other pathways to influence mineralized tissue development. Specifically, studies using *Tgfbr2* loss of function animal models suggest a critical role during the development of structures (*eg*, teeth, jaw, and cranial skeleton) that impact overall craniofacial morphology. Phenotypic observations include cleft palate, absent or defective calvaria components, reduced and/or defective mandibular process morphology, abnormal molar root, and abnormal dentin formation.[6-11]

Mesenchymal cells are multipotent cells that, upon differentiation, contribute to multiple craniofacial structures including bones and teeth. Commitment to a bone-forming osteoblastic or dentin-forming odontoblastic lineage corresponds with the expression of Osterix/ SP7 (*Osx*), a transcription factor that restricts chondrogenic differentiation and acts downstream of Runx2, another key regulator of bone formation.[12] Despite critical spatial, functional, and gene expression differences between mature osteoblasts and odontoblasts, *Cre* recombinase expression driven by the *Osx* promoter allows targeted gene knockout in immature, but committed, mineralized tissue forming cells.[13] Such *Osx-Cre* recombinase-based excisional approaches also circumvent perinatal lethality issues observed in other tissue specific conditional knockout models thereby allowing investigation into gene function and craniofacial morphology at postnatal time points.[6,8] Multiple studies documented that *Osx-Cre*-mediated *Tgfbr2* deletion leads to shortened molar root, hypomorphic cementum, and reduced bone volume and bone density.[11,14,15]

In the present study, using mice with *Osx-Cre*-mediated *Tgfbr2* deletion, we focus our studies in 3D morphology to highlight insight into the etiology of anomalous craniofacial states, which have not been characterized. Our analyses at postnatal day 26 correspond to near-maximal skull growth and indicate that *Tgfbr2* affects anterior skull, palate, skull base, mandibular, and molar root morphology. These results critically corroborate the craniofacial phenotypic outcomes of conditional *Osx-Cre*-mediated *Tgfbr2* deletion reported in other studies[9,11] while also highlighting a useful method for quantitatively comparing the 3D morphology of mineralized structures.

2 | MATERIALS AND METHODS

2.1 | Animal model

All animals and experiments were performed in accordance with the policies and federal laws for the judicious use of vertebrate animals, as approved by the University Committee on Use and Care of Animals at the University of Michigan. Conditional knockout mice for *Tgfbr2* were generated through Cre-lox recombination driven by the *Osx* promoter. Mice that did not carry the *Osx-Cre* transgene (*ie*, *Osx-Cre⁻*), and therefore did not have *Tgfbr2* deletions, were designated

as "control" animals and compared against their *Osx-Cre⁺* (conditional knockout or "cKO") littermates. All analyses were performed at postnatal day 26 (P26).

2.2 | Micro-CT (μCT)

Micro-CT scanning of fixed heads was performed at the University of Michigan using a Micro-CT core (μCT40 Scanco Medical, Bassersdorf, Switzerland). Scan settings were the following: voxel size 18 μm, 55 kVp, 109 μA, 0.5 mm AL filter, and integration time 500 ms.

2.3 | Image analysis

Structures of interest were segmented and converted to 3D mesh models from micro-CT data using ITK-SNAP (itksnap.org, open source software developed by grants and contracts from the United States National Institutes of Health). Shape comparisons against a single reference model (*ie*, control mouse structure/s of interest) were then performed using tools developed in 3D Slicer (slicer.org, open source software). Briefly, landmarks (see Tables 1-3) were placed ("CMF Reg tool") thereby allowing for model superimposition based on the minimization of Euclidean distance between similar surface points. The distances between corresponding landmarks were measured using the "Q3DC tool." The distances between closest points on the model surfaces were also calculated using "Model to Model Distance tool" which were then used to generate a heatmap ("Shape Population Viewer tool") that illustrated regions/surfaces which differed from the reference model based on point to point alignment.

3 | RESULTS

3.1 | Craniofacial dysmorphism is observed in Tgfbr2^fl/fl/Osx-Cre mice

Disruption of *Tgfbr2* by *Osx-Cre* resulted in altered craniofacial morphology that was apparent at P26. Most pronounced were reductions in skull and incisor size, the latter of which appeared either missing

TABLE 1 Mandibular landmarks used to superimpose digital models and generate heatmaps in Figure 3

Point 1	Most anterior point on alveolus
Point 2	Most superior, posterior condyle
Point 3	Most distal point on angular process
Point 4	Most superior point on coronoid process
Point 5	Most superior point of antegonial notch
Point 6	Distal point of molar alveolus
Point 7	Anterior point of molar alveolus
Point 8	Greatest concavity along posterior border

TABLE 2 Cranial base landmarks used to superimpose digital models and generate heatmaps in Figure 4

Point 1	Most anterior point of the indentation in the center of the presphenoid
Point 2	Most anterior point on the anterior projection on the presphenoid
Point 3	Posteromedial point of the inferior portion of the left alisphenoid
Point 4	Most anterolateral point on corner of the basioccipital at the basioccipital synchondrosis
Point 5	Mid-point on the anterior margin of the foramen magnum, taken on squamosal occipital
Point 6	Most inferolateral point on the squamous occipital
Point 7	Mid-point on the posterior margin of the foramen magnum, taken on basioccipital

or unerupted upon initial inspection (Figure 1A-H). Tomographic and lateral radiographic analysis confirmed the presence of diminutive upper and lower incisors which likely contributed to an anterior open bite phenotype (Figure 1C,D,G-I). Also apparent was posterior widening of the interfrontal suture and porosities within the frontal bone suggestive of lower mineral content (Figure 1I). Although these collective phenotypic differences indicate changes in the anterior facial morphology of cKO mice, the inability to localize specific regions of change represents a limitation of two-dimensional (2D) cephalometric analysis. We therefore employed qualitative 3D whole skull alignment which both highlighted anteroposterior skull shortening and implicated deficiencies within structures anterior of the coronal suture (Figure 1J).

3.2 | Anterior skull defects are observed in Tgfbr2$^{fl/fl}$/Osx-Cre mice

Shape-based 3D analysis indicated a high degree of morphologic difference in anterior regions of cKO mouse skulls (Figure 2, top). Whole skull superimposition revealed that the area surrounding the intersection of the frontonasal and interfrontal sutures was a "hotspot" of morphologic change (Figure 2, middle). Likewise, significant changes in shape were seen in the maxilla and became progressively worse when moving anterior from the transverse palatine suture (Figure 2, bottom). Importantly, these observations (ie, differences along sutures within the anterior facial region) corroborated those from our 2D analysis thereby supporting quantitative 3D analysis as an improved method for assessing phenotypic changes. Despite its utility

TABLE 3 Mandibular molar landmarks used to superimpose digital models and generate heatmaps in Figure 5

Point 1	Middle buccal surface
Point 2	Middle lingual surface
Point 3	Mesial contact point
Point 4	Distal contact point
Point 5	Mesiobuccal cusp tip
Point 6	Distobuccal cusp tip
Point 7	Mesiobuccal root apex
Point 8	Distobuccal root apex

in shape-based data visualization, a limitation of this technique can also be seen along the zygomatic arch which, due to its long, narrow shape, is sensitive to model superimposition (Figure 2, bottom).

3.3 | Morphologic differences are present along the mandibular periphery in Tgfbr2$^{fl/fl}$/Osx-Cre mice

Broad differences in craniofacial appearance (eg, facial profile) are affected by the size, shape, and position of skull components. Besides the ossicles of the inner ear, the mandible is the only mobile skull bone and plays a critical role in both mastication and the determination of facial profile. Shape-based analyses of cKO mice validated suspicions of shortened mandibles and revealed deficiencies at the condyloid process, coronoid process, angular process, and incisor alveolus (Figure 3). Despite reductions in overall jaw size, these structures were not grossly misshapen in cKO mice. Rather, the position of these structures along the periphery of the mandible and the proportional but scaled-down appearance of the mandible indicated impaired growth following *Tgfbr2* disruption.

3.4 | Anterior skull length is shorter, but skull base morphology is not significantly affected in Tgfbr2$^{fl/fl}$/Osx-Cre mice

The skull base is a midline structure that connects the facial skeleton with posterior elements of the skull and aberrant skull base morphology has been found to contribute to other syndromic facies. Analysis of the skull base revealed that skull base is proportionally shorter as if scaled down to the smaller skull size in the cKO mice (Figure 4A,B). Differences in skull morphology and facial profile were therefore due to differences in the anterior skull (eg, facial skeleton and palate) and not secondary effects (ie, restricted anterior and superior growth of the facial skeleton) of disproportional skull base shortening. However, although shape-based analyses seemingly indicate differences along the presphenoid and anterior portions of the greater wings of the sphenoid, these can be disregarded and attributed to an inherent limitation during image segmentation; tomographic image resolution restricts differentiation of fine anatomic structures. As such, "hotspots" were
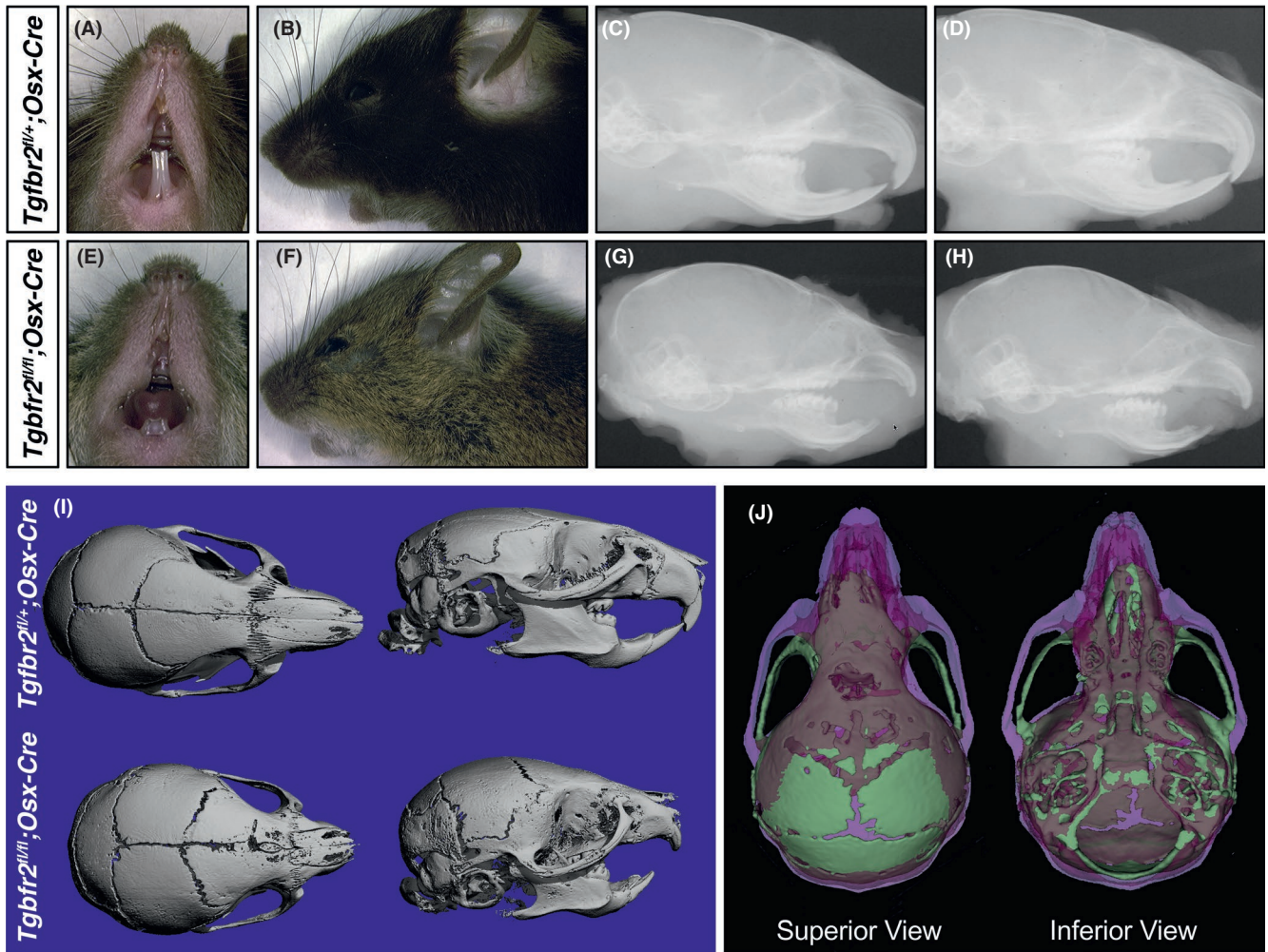
FIGURE 1 Comparison of gross craniofacial morphology. (A-H) External morphology and lateral cephalometric radiography. *Tgfbr2*-cKO mice (bottom, E-H) had reduced anterior-posterior skull length and erupted incisor length at postnatal day 26 (P26). Noted findings were diminished skull size and an anterior open bite in *Tgfbr2*-cKO mice. (I) Whole skull tomographic imaging confirmed the presence of diminutive upper and lower incisors and suggested potential shortening of the jaws and the presence of interfrontal suture pathology in *Tgfbr2*-cKO mice. (J) Whole skull tomographic imaging-based comparison of craniofacial morphology. Posterior alignment of whole Control vs *Tgfbr2*-cKO (purple vs green, respectively) skulls illustrated differences in overall size and the morphology of facial skeletal structures

seen along the periphery of anterior structures in both control and cKO mice (Figure 4C).

3.5 | Molar root morphology is more affected than the crowns in Tgfbr2fl/fl/Osx-Cre mice

Facial height, and therefore appearance, is a byproduct of mandibular morphology (*eg*, mandibular angle) and vertical dimension of occlusion (VDO), the superior-inferior relationship of the jaws. VDO is determined by tooth size and alignment as this space in dentate organisms is primarily occupied by the crowns of molar teeth. Crown surface features (*ie*, cusps, ridges, and fossae) are highly complex and harmonious inter-arch relationship exists when there is interposition of these features. Analysis of mandibular first and second molars revealed that shape-based differences in cKO mouse molars were more pronounced at the root apices compared to the crowns (Figure 5A,B). Therefore, craniofacial morphological differences are

FIGURE 2 Shape-based three-dimensional comparison of whole skull morphology. (Top) Heatmaps generated from shape-based comparisons of entire skulls indicated "hotspots" of change located in the anterior skulls of *Tgfbr2*-cKO mice (bottom row). (Middle) Magnified views of the interfrontal suture and anterior skull regions that exhibited significant morphologic dissimilarity. (Bottom) Magnified views of the transverse palatine suture and palatal regions that exhibited significant morphologic dissimilarity. Green indicates morphologic similarity (*ie*, no change) whereas warm (*eg*, yellow-to-red) and cool (*eg*, cyan-to-violet) colors indicate the degree of reduction or increase, respectively, in Euclidean distances between similar surface points. A single control mouse (*ie*, Ct 4) was used as reference to generate the comparative heatmaps for control samples (*ie*, Ct 1 through 4; top rows) and *Tgfbr2*-cKO samples (*ie*, mt 1 through 4; bottom rows) in each panel
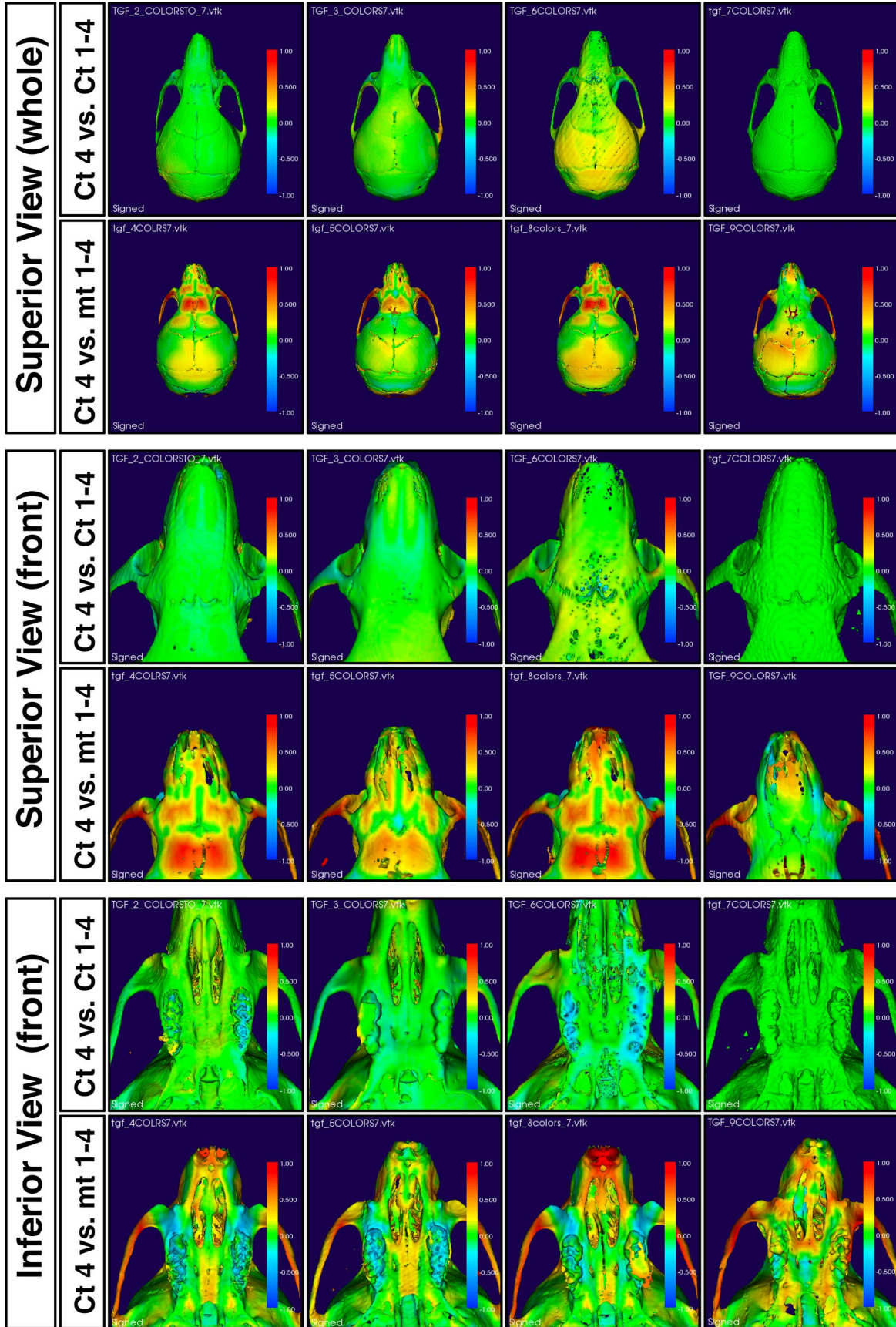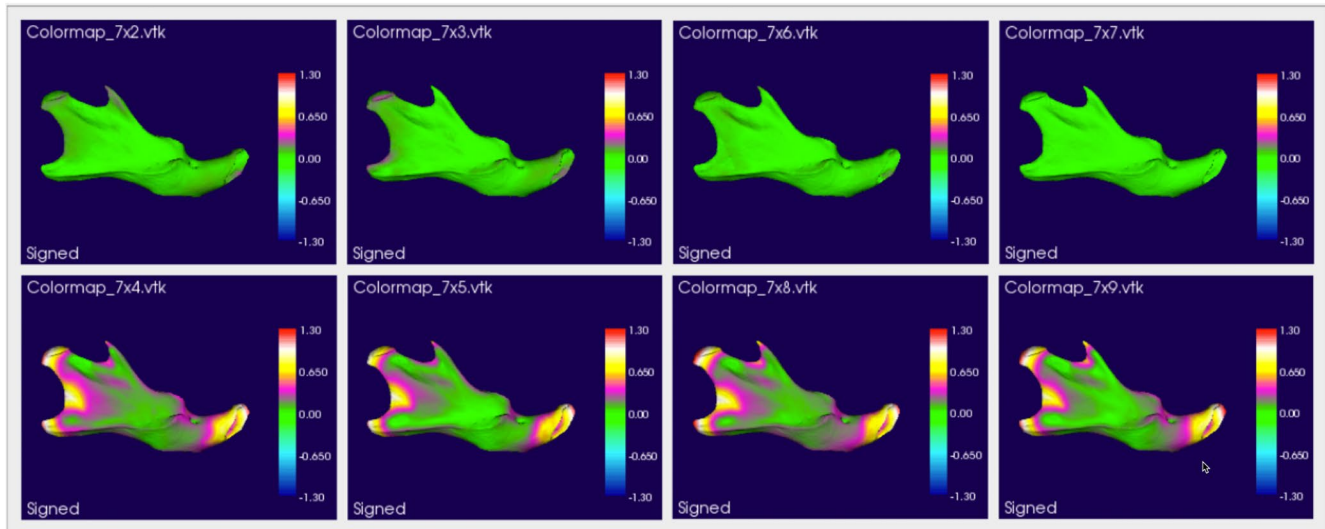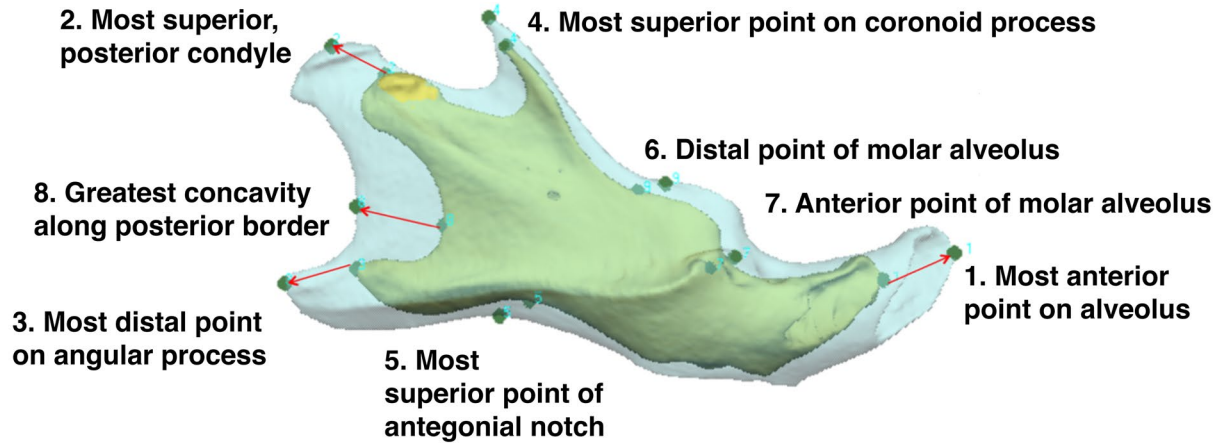
FIGURE 3 Comparison of mandibular morphology. Heatmaps generated from shape-based mandibular comparisons reflect observations of reduced lower jaw size in *Tgfbr2*-cKO mice (bottom row) compared to control counterparts (top row). "Hotspots" of significantly dissimilar morphology (ie, regions colored purple and yellow) were located along the periphery and include the condyloid process, coronoid process, angular process, and incisor alveolus. Green indicates morphologic similarity (ie, no change) whereas warm (eg, fuchsia-to-red) and cool (eg, cyan-to-violet) colors indicate reduction or increase, respectively, in Euclidean distances between similar surface points. A single control mouse (ie, Sample ID 7) was used as reference to generate the comparative heatmaps for control samples (ie, Sample IDs 2, 3, 6, 7; top rows) and *Tgfbr2*-cKO samples (ie, Sample IDs 4, 5, 8, 9; bottom rows) in each panel

driven by skull elements and not coronal dysmorphism. Whether *Tgfbr2* plays a direct role in root elongation or if the root phenotype observed in this study represents outcomes of cell (ie, odontoblast and bone producing mesenchyme) interactions cannot be determined using the current model and 3D analytic technique.

4 | DISCUSSION

Multiple previous studies demonstrated that *Osx-Cre*-mediated *Tgfbr2* deletion leads to various types of abnormalities in mineralized tissues. With most of previous histological analysis being focused on the mechanism leading to abnormal odontoblast and osteoblast differentiation, our 3D morphological analysis provides a complementing insight into the etiology of anomalous craniofacial states.[11,14,15] Model segmentation and digital superimposition from tomographic

imaging allows for the unbiased, 3D shape-based comparison of structures of interest. Such analyses provide detailed insight regarding regions or sources underlying abnormal craniofacial morphology beyond the capabilities of standard cephalometric tracing and analysis.[1,2] While tomographic imaging (eg, cone beam CT) has become more common in clinical dentistry, increased radiation exposure and the high cost of imaging equipment limits 3D analysis to either small areas of interest (eg, single teeth) or cases involving extensive surgical reconstruction. Despite inherent limitations related to image resolution, comparative heatmaps based on superimposed models provide quantitative, straightforward, and visually attractive representations of morphology-based data.

Gross phenotypic differences (ie, anterior open bite and reduced overall skull size) observed in *Tgfbr2*^{fl/fl}/*Osx-Cre* cKO mice are attributable to small incisor size and disruption of structures/regions proximal to the nasofrontal, interfrontal, and transverse palatine sutures. This
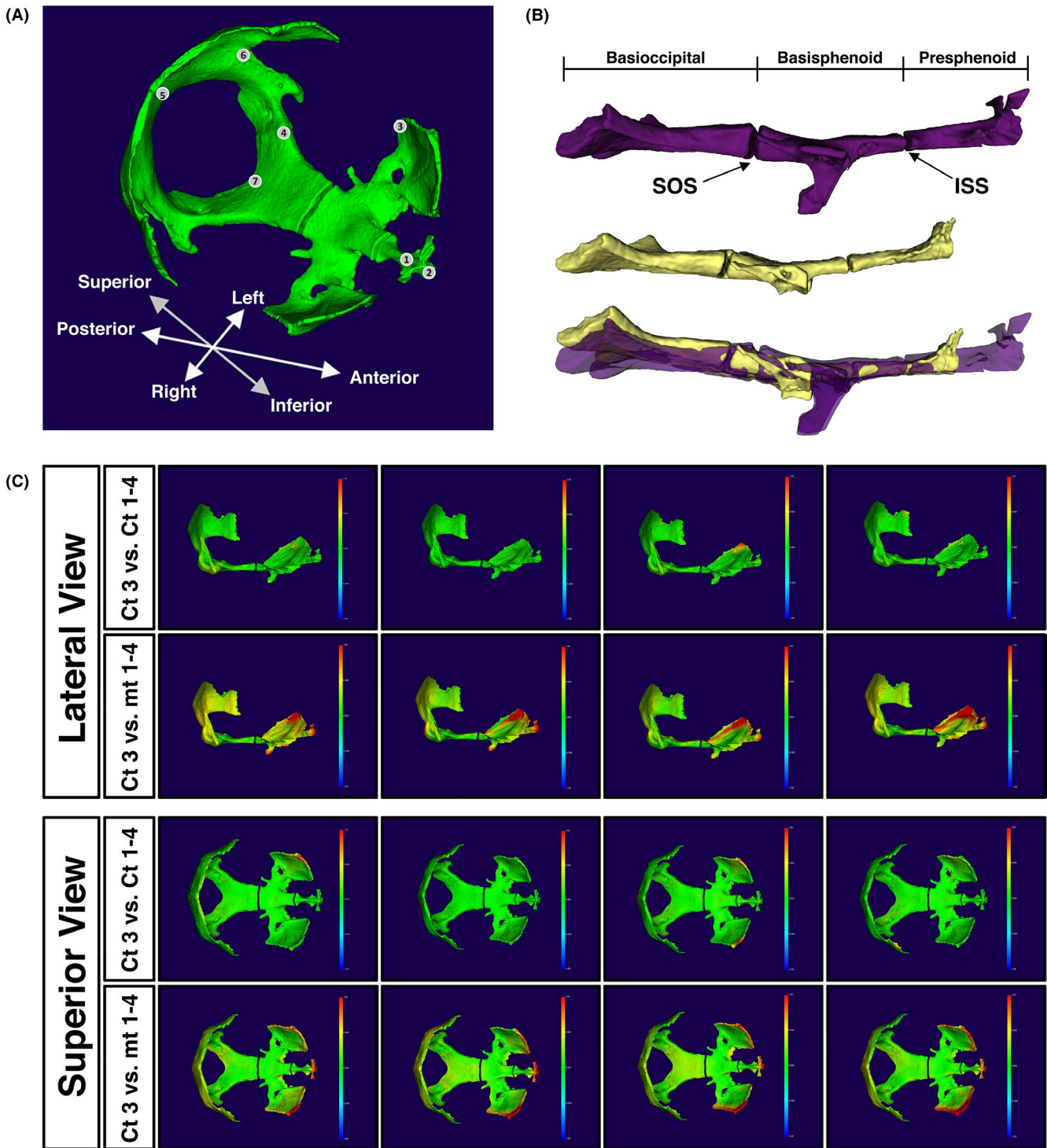
FIGURE 4 Comparison of skull base morphology. (A) Representative skull base with landmarks corresponding to those listed in Table 2. (B) Magnified overlay of elements defining the inferior skull base indicated proportional shortening of the skull base in *Tgfbr2*-cKO mice (yellow). Structures are bound by points 1, 2, 4, and 7 shown in Table 2 and Figure 4A. Spheno-occipital synchondrosis (SOS) is located between the basioccipital and basisphenoid. Intersphenoid synchondrosis (ISS) is located between the basisphenoid and presphenoid. (C) Heatmaps generated from shape-based comparisons of skull base morphology between Control and *Tgfbr2*-cKO mice (top vs bottom row, respectively) illustrated differences along the anterior wings of the alisphenoid. Green indicates morphologic similarity (ie, no change) whereas warm (eg, yellow-to-red) and cool (eg, cyan-to-violet) colors indicate reduction or increase, respectively, in Euclidean distances between similar surface points. A single control mouse (ie, Ct 3) was used as reference to generate the comparative heatmaps for control samples (ie, Ct 1 through 4; top rows) and *Tgfbr2*-cKO samples (ie, mt 1 through 4; bottom rows) in each panel
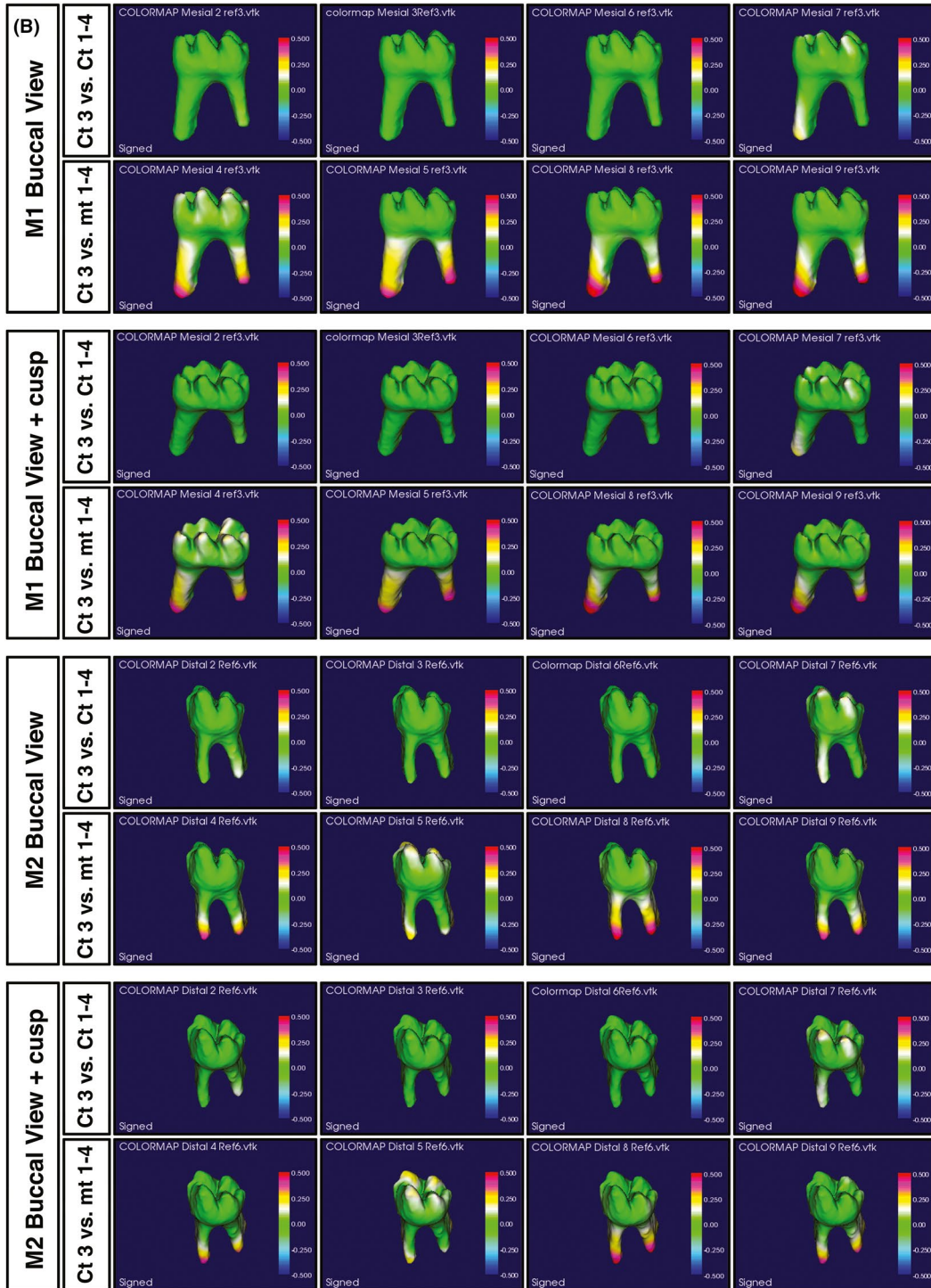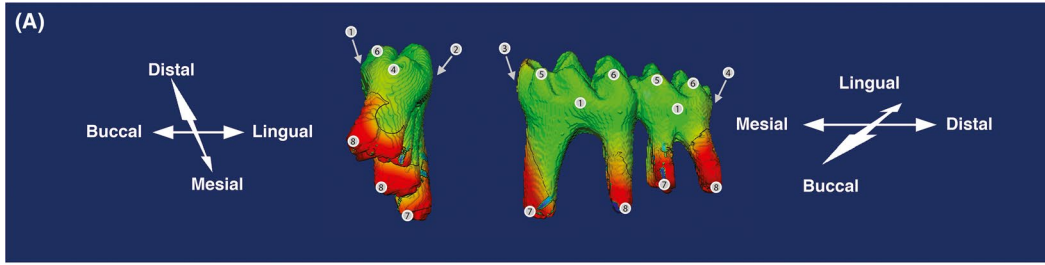
FIGURE 5 Comparison of mandibular molar morphology. (A) Representative molars with landmarks corresponding to those listed in Table 3. (B) Heatmaps generated from shape-based comparisons of molar morphology between Control and *Tgfbr2*-cKO mice highlighted differences in root length. Non-significant differences in coronal features were observed. Green indicates morphologic similarity (ie, no change) whereas warm (eg, yellow-to-red) and cool (eg, cyan-to-violet) colors indicate reduction or increase, respectively, in Euclidean distances between similar surface points. A single control mouse (ie, Ct 3) was used as reference to generate the comparative heatmaps for control samples (ie, Ct 1 through 4; top rows) and *Tgfbr2*-cKO samples (ie, mt 1 through 4; bottom rows) in each panel

suggests that *Tgfbr2* may influence overall craniofacial morphology by maintaining suture patency and supporting growth in the anterior facial region. These observations were critical findings of the present study because: (a) small, non-occluding incisors and skulls were consistent with other studies using a similar *Tgfbr2*^{fl/fl}/*Osx-Cre* cKO mouse model[9,11] and (b) the application of our shape-based analysis permitted identification of specific craniofacial regions with morphologic dissimilarities. It was noted by previous studies that *Tgfbr2*^{fl/fl}/*Osx-Cre* cKO mice have normal size of the skull and mandible at the new born stage.[11] Therefore, the noted small skull and mandible are due to affected postnatal growth due to *Tgfbr2* loss of function. In previous studies, *Tgfbr2*^{fl/fl}/*Osx-Cre* cKO mice develop dwarfism due to the decrease chondrocyte proliferation in the growth plate .[11] Given that skull base elongation is through endochondral ossification, the shortened skull base in *Tgfbr2*^{fl/fl}/*Osx-Cre* cKO is likely due to the decreased chondrocyte proliferation in two synchondroses of the skull base. *Tgfbr2* loss of function mediated by *Osx-Cre* leads to decreased proliferation and slow maturation of pre-osteoblast,[11] which is not directly helpful to explain the small skull and mandible. Cranial sutures serve as signaling centers for skull bone growth and their premature fusion restricts postnatal calvaria growth, a hallmark of craniosynostosis[16] and the mechanism controlling mandible growth remains elusive. Although sutures in *Tgfbr2*^{fl/fl}/*Osx-Cre* cKO mice were not histologically evaluated to confirm premature fusion, we would expect craniosynostosis due to the known contribution of reduced TGF-β signaling in premature suture fusion[17,18] and the craniofacial signs (ie, craniosynostosis and abnormal palatal shape) in patients with Loeys-Dietz syndrome, a condition associated with *TGFBR2* mutations.[4,15] Additionally, *Tgfbr2* is expressed in both cranial sutures and developing tooth buds thereby suggesting potential involvement in their development.[19] Patients with Loeys-Dietz syndrome are also described as having dental findings including malocclusions, dental crowding, affected mandibular projection, and delayed eruption of permanent incisors, all traits which could affect facial profile and contribute to an anterior open bite similar to observations in mice.

Like reduced skull and incisor size, molar root dysmorphism is a consistent characteristic of *Tgfbr2*^{fl/fl}/*Osx-Cre* cKO mice.[11] Tooth formation requires spatiotemporally coordinated interaction between cells of different origin (ie, epithelium-derived ameloblasts and mesenchyme-derived odontoblasts) and root formation initiates (postnatally in mice) after crown completion.[20,21] This process involves coordination of both enamel epithelium, Hertwig's epithelial root sheath (HERS) and mesenchyme. Root growth begins with the apical migration and fusion of the inner and outer enamel epithelium into HERS. The epithelial derived HERS subsequently affects root morphology as well as root dentin formation through its interaction with mesenchymal cells of the dental papilla. It was documented

previously that *Tgfbr2*^{fl/fl}/*Osx-Cre* cKO mice have delayed elongation and disorganization in HERS.[11] Since *Osx-Cre* target into mesenchyme of tooth, the affected HERS is secondarily due to the affected odontoblast differentiation. In our study, the morphological analysis showcases the short, dysmorphic molar roots in *Tgfbr2*^{fl/fl}/*Osx-Cre* cKO mice suggesting that *Tgfbr2* in committed odontoblasts within the dental papilla is important for postnatal root elongation and dentin development. This influence of *Tgfbr2* on dentin development and tooth morphology is further supported by observations of dysmorphic crown dentin formation in alternative *Tgfbr2*-cKO mouse models.[6,8]

Osx is expressed as early as E13.5.[12,13] Our conditional gene knockout should, presumably, result in reduced TGF-β signaling before the birth in all *Osx*-expressing skull components and coronal and radicular dentin. However, we believe that *Tgfbr2* plays important roles during postnatal mineralized tissue formation because morphologically affected regions undergo significant growth and development after birth. As previously discussed, root formation is a postnatal (through approximately P26) event in mice and differences were seen in root but not crown morphology. Similarly, the murine facial skeleton during the first month of life grows more relative to the cranium and was another "hotspot" of morphologic difference.[22] Conversely, we did not see significant differences in skull base morphology, a region with proportionality little anterior-posterior growth through P30. *Tgfbr2* in *Osx*-expressing cells was also found to be dispensable during prenatal but not postnatal femur growth.[15] We therefore believe that morphologic differences reflect postnatal-specific differences caused by *Tgfbr2* deficiency and not a secondary effect of the *Osx* promoter used to drive Cre recombinase-based excision.

5 | CONCLUSION

We hereby present findings that corroborate and expand upon prior findings using a similar *Tgfbr2*^{fl/fl}/*Osx-Cre* cKO mouse model by identifying specific regions of morphologic change in the anterior skull, mandible, and molar roots. Superimposition of 3D models constructed from tomographic imaging presents a useful tool for determining the etiology of changes to craniofacial morphology and application of this technique critically expounds the role of *Tgfbr2* during postnatal development of mineralized tissues in the craniofacial region.

CONFLICT OF INTEREST

All authors declare no conflict of interest.

ORCID

Yuji Mishina 🆔 https://orcid.org/0000-0002-6268-4204

REFERENCES

1. Wen J, Liu S, Ye X, Xie X, Li J, Li H, et al. Comparative study of cephalometric measurements using 3 imaging modalities. J Am Dent Assoc. 2017;148:913–21.
2. Kumar V, Ludlow JB, Mol A, Cevidanes L. Comparison of conventional and cone beam CT synthesized cephalograms. Dentomaxillofacial Radiol. 2007;36:263–9.
3. Loeys BL, Chen J, Neptune ER, Judge DP, Podowski M, Holm T, et al. A syndrome of altered cardiovascular, craniofacial, neurocognitive and skeletal development caused by mutations in TGFBR1 or TGFBR2. Nat Genet. 2005;37:275–81.
4. Jani P, Nguyen QC, Almpani K, Keyvanfar C, Mishra R, Liberton D, et al. Severity of oro-dental anomalies in Loeys-Dietz syndrome segregates by gene mutation. J Med Genet. 2020;57(10):699–707.
5. Massagué J. TGF- β SIGNAL TRANSDUCTION. Annu Rev Biochem. 1998;67:753–91.
6. Ito Y, Yeo JY, Chytil A, Han J, Bringas P, Nakajima A, et al. Conditional inactivation of Tgfbr2 in cranial neural crest causes cleft palate and calvaria defects. Development. 2003;130:5269–80.
7. Oka K, Oka S, Hosokawa R, Bringas P Jr, Brockhoff HC II, Nonaka K, et al. TGF-β mediated Dlx5 signaling plays a crucial role in osteo-chondroprogenitor cell lineage determination during mandible development. Dev Biol. 2008;321:303–9.
8. Oka S, Oka K, Xu X, Sasaki T, Bringas P Jr, Chai Y. Cell autonomous requirement for TGF-β signaling during odontoblast differentiation and dentin matrix formation. Mech Dev. 2007;124:409–15.
9. Seo H-S, Serra R. Tgfbr2 is required for development of the skull vault. Dev Biol. 2009;334:481–90.
10. Nakamura T, Colbert MC, Robbins J. Neural crest cells retain multipotential characteristics in the developing valves and label the cardiac conduction system. Circ Res. 2006;98:1547–54.
11. Wang Y, Cox MK, Coricor G, MacDougall M, Serra R. Inactivation of Tgfbr2 in Osterix-Cre expressing Dental Mesenchyme Disrupts Molar Root Formation. Dev Biol. 2013;382:27–37.
12. Nakashima K, Zhou X, Kunkel G, Zhang Z, Deng JM, Behringer RR, et al. The Novel Zinc Finger-Containing Transcription Factor Osterix Is Required for Osteoblast Differentiation and Bone Formation. Cell. 2002;108:17–29.
13. Rodda SJ, McMahon AP. Distinct roles for Hedgehog and caronical Wnt signaling in specification, differentiation and maintenance of osteoblast progenitors. Development. 2006;133:3231–44.
14. Choi H, Ahn Y-H, Kim T-H, Bae C-H, Lee J-C, You H-K, et al. TGF-β Signaling Regulates Cementum Formation through Osterix Expression. Sci Rep. 2016;6:1–11.
15. Peters SB, Wang Y, Serra R. Tgfbr2 is required in osterix expressing cells for postnatal skeletal development. Bone. 2017;97:54–64.
16. Twigg SRF, Wilkie AOM. A Genetic-Pathophysiological Framework for Craniosynostosis. Am J Hum Genet. 2015;97:359–77.
17. Opperman LA, Adab K, Gakunga PT. Transforming growth factor-β2 and TGF-β3 regulate fetal rat cranial suture morphogenesis by regulating rates of cell proliferation and apoptosis. Dev Dyn. 2000;219:237–47.
18. Sanford LP, Ormsby I, Gittenberger-de Groot AC, Sariola H, Friedman R, Boivin GP, et al. TGF-beta 2 knockout mice have multiple developmental defects that are non-overlapping with other TGF-beta knockout phenotypes. Development. 1997;124:2659–70.
19. Wang Y, Sizeland A, Wang X, Sassoon D. Restricted expression of type-II TGFP receptor in murine embryonic development suggests a central role in tissue modeling and CNS patterning. Mech Dev. 1995;52:275–89.
20. Thesleff I, Nieminen P. Tooth morphogenesis and cell differentiation. Curr Opin Cell Biol. 1996;8:844–50.
21. Lungová V, Radlanski RJ, Tucker AS, Renz H, Míšek I, Matalová E. Tooth-bone morphogenesis during postnatal stages of mouse first molar development. J Anat. 2011;218:699–716.
22. Wei X, Thomas N, Hatch NE, Hu M, Liu F. Postnatal craniofacial skeletal development of female C57BL/6NCrl mice. Front Physiol. 2017;8:1–18.